SSRG International Journal of Electrical and Electronics Engineering
ISSN: 2348-8379/ https://doi.org/10.14445/23488379/IJEEE-V11I5P117

Volume 11 Issue 5, 188-198, May 2024


*Original Article*

# Single-Switch Inverter Design for Reduced Losses and Improved PV-Grid Integration

Sivaraj Panneerselvam[1], Karunanithi Kandhasamy[2]

[1,2]*Department of EEE, Vel Tech Rangarajan Dr. Sagunthala R&D Institute of Science and Technology, Tamil Nadu, India.*

[1]*Corresponding Author : psivaraj@veltech.edu.in*

Received: 11 March 2024 Revised: 11 April 2024 Accepted: 09 May 2024 Published: 29 May 2024

***Abstract*** - *Photovoltaic (PV) renewable power generation is becoming increasingly common in industrial and household applications. However, these sources of renewable energy can cause environmental damage, increase power demand, and result in various losses due to interactions between converters and inverters. To address these issues, a proposed solution is to use a Photovoltaic (PV) input source tracking-based MPPT using CNN with switching operation and an output inverter connected to the grid. A battery is also included for backup to charge and discharge the input DC voltage. Voltage levels may be adjusted with this non-isolated DC/DC converter by using its buck and buck-boost modes. By balancing the input source, the non-isolated DC/DC converter connects the MOSFET switches based on the Selective Harmonic Elimination condition to reduce power loss and conduction loss by utilizing a switch device. The MOSFET switches operate at the fundamental frequency to achieve high voltage conversion in the VSI DC/AC inverter. The output results are analyzed through MATLAB simulation to determine the voltage drop and power loss across the switches.*

***Keywords*** - *Photovoltaic (PV), Metal Oxide Semiconductor Field Effect Transistors (MOSFETS), Conduction loss, Power losses, Maximum Power Point Tracking (MPPT), Convolutional Neural Network (CNN).*

## 1. Introduction

Photovoltaic power sources experience various losses, including power and conduction losses. Weather conditions cause these losses to affect the surface of photovoltaic panels and the energy conversion process. A non-isolated DC-DC boost converter must raise the DC voltage from low to high in order to solve this problem. Both active and passive parts, including transistors, inductors, diodes, and capacitors, are used in this converter. This is accomplished by varying the Pulse Width Modulator's (PWM) duty cycle in order to feed the inductor and capacitor.

Photovoltaic energy works in two ways: as a separate system consisting of a photo array, a battery, and a grid-connected system that consists of a photovoltaic array and as an inverter with a particular technology. According to current conditions and development patterns, independent photovoltaic arrays will continue to dominate the use of solar energy for photovoltaic electricity, even with the rise of grid-connected systems. In distant or remote areas where the electricity grid is not accessible, standalone battery packs.

Voltage conversions are becoming increasingly significant for a range of commercial uses. The decrease in semiconductor switches and the devices' ability to work at high frequencies are two causes of this issue. The power converter output must satisfy the load parameters for the system to function adequately—a DC-DC converter output voltage ripples caused by an innate parasitic element in the switching unit. The system's stability, effectiveness, and performance may all suffer as an outcome. Therefore, a lossless filter is employed as the interface between the load and the converter to reduce this effect. As an outcome, factors such as shadowing and climate change can significantly impact the power output (current and voltage) from PV panels.

When the inverter devices are turned off, the MOSFET switches reduce voltage spikes and regenerate the connected inductor leakage energy. The Voltage Source Inverters (VSIs) are compared with current configurations by considering variables theoretically derived from steady-state evaluations of voltage gain. Voltage gain and voltage load between the diode and the valve. These converters can be divided into two categories: bonded inductors and switches.

## 2. Literature Review

Low-Voltage (LV) power quality concerns were investigated at Conventional Connecting Points (PCCs), including significant nonlinear loads. To assess the PCC's seasonal variations and total harmonic distortion of voltage (THDv) and current (THDi), a radially rebuilt IEEE-34 bus system was employed.

The solar PV penetration rate was simulated under multiple scenarios (ranging from ~100%). investigate. Apply actionable feed data in a poor grid setting. The findings indicate that 50% solar PV integration decreases active, reactive, and perceived power losses by 1.9%, 2.6%, and 3.3%, respectively. This is due to the grid's enhanced voltage profile as compared to the baseline scenario with no solar energy. Furthermore, THDi and THDv at PCC were measured to be 10.2% and 5.2%, respectively, at 50% PV penetration [1].

A comprehensive investigation of Double-Coupled Photovoltaic (DCPV) systems, with an emphasis on increasing power quality and developing dependable operating methods. This system employs a DC-DC power converter to maintain the alternating DC voltage and a voltage converter to convert the stable DC voltage to AC voltage. The LCL filter employed in this test reduced the network voltage THD from 0.59% to 0.08%, the network output current THD from 10.71% to 1.17%, and the THD inverter current from 10.70% to 4.9 percent. This translates to a 10x increase in power usage over a system without a filter element [2].

The work compares soft computing MPPT approaches for Particle Swarm Optimum (PSO), Variable Step Size Radial Basis Function Algorithm (VSS-RBFA), Fixed Step Size Radial Basis Function Algorithm (FSS-RBFA), and Cuckoo Search (CS). The evaluation takes into account algorithm complexity, tracking speed, MPP fluctuation, and acquisition factors in both static and dynamic irradiation scenarios. The maximum power dissipation and Fill Factor (FF) of the single and dual-diode PV module variants are also assessed [3].

In this situation, the solar inverter serves as the primary link between the solar power plant and the utility. These inverters are critical components in solar power systems. Due to the constraints of microgrid systems, single-phase inverters are employed for domestic power generation and grid connection. This contrasts with the three-phase converters employed in large-scale Photovoltaic (PV) applications.

Control techniques for single-phase and multi-phase single-phase converters have been thoroughly investigated, and the development of DC-DC converters and inverter topologies has been evaluated. Various isolated and non-switched circuit topologies are investigated with commercial and test equipment [4].

The artificial bee colony approach may be used to track Maximum Power Points (MPPT) in PV systems powered by DC-DC converters. This approach uses the PV module's data values to derive the PV attributes and ideal voltages. MPPT technology is then applied to get a voltage reference from an external PI control loop, which serves as a current reference for predictive power electronics module control. The hardware-in-the-loop solution includes a Digital Signal Controller (DSC) and a High-Speed Flight Simulator (PLECS RT Box 1). The findings produced using this procedure are quite accurate. Furthermore, all functionalities may be implemented at a minimal cost by applying a consumer DSC (TI 28069M) [5].

The IGWO algorithm for solar systems' Maximum Power Point (MPPT) under environmental and dynamic Protection Conditions (PSC). The findings are compared to various MPPT algorithms, such as Enhanced GWO (EGWO), Grey Wolf Optimizer's Slaps Algorithm (SSA-GWO), Artificial Bee Colony algorithm (ABC), Perturbed and Observed algorithm (P&O), and PSO.

The suggested control technique has been validated as stable and efficient, particularly for monitoring speed under PSC. The simulation results reveal that the IGWO algorithm paired with the BFBIC topology outperforms the other methods in most circumstances. In fact, our approach needs just 0.24 seconds of monitoring time and delivers 98.54% efficiency in the most demanding PSC [6].

The two phases of the process are the calculation and the calibration phases. Both fine and rough positioning functions are included in the statistical section. The regulation area uses small components to regulate the DC-DC converter's cycle of operation, thereby increasing the monitoring efficiency. In addition, computerization helps shorten reaction times. Because of the unstable nature of photo arrays, the MPPT method is used to ensure that they continue to perform at their maximum potential [7].

The low efficiency of the power conversion of multi-level inverters can be improved by using asymmetric multi-level transformers. The advantage is that it has fewer components while providing the same output as a multi-level converter with less harmonic distortion (THD). This study proposes a new design for an asymmetric multi-level converter and presents an example of a control phase switching method.

An important feature of this configuration is the use of 86% fewer switching devices compared to a normal-level H-bridge converter because 87% fewer switching devices are needed for one phase of seven production units. The proposed architecture is similar to existing symmetrical designs in terms of characteristics such as THD, cost, weight, and power consumption. The results show that this topology reduces system weight and hardware costs by 23.89% and 23.57% compared to the existing design. In addition, THD is reduced by 2.43% in Asymmetric-1 and 4.37% in Asymmetric-2 [8].

A DC-DC power converter (HVGSU) for use with Peak Power Collectors (MPP) in photovoltaic systems. Using DC-DC converters, photovoltaic arrays can provide power by increasing the output voltage to meet demand. Since the solar power is variable, the PV array should be operated below the

MPP using the MPPT control method. The present study presents a basic HVGSU converter that incorporates a voltage multiplier unit with a switching capacitor and a main boost converter device. The architecture can be combined and integrated to enable high voltage step-up and monitor power signals so that the control network can change voltages from 20-40 V to 380 V at 150 W [9].

A comparative was conducted on MG PV/DC wind buses combining battery storage and SMES systems. The FLC method is proposed to operate batteries and SMEs efficiently. To reduce the load voltage/frequency, the main converter uses variable control technology.

The control system's performance is examined under substantial and frequent weight fluctuations, as well as various weather situations. The findings indicate that the SMES system outperforms the battery in all of the variants examined. The suggested FLC approach is based on monitoring the current in the battery and SMES and detecting the variations in the DC bus voltage [10].

Microgrids are systems that operate independently and are not connected to the power grid. To handle photovoltaic power generation, several DC-DC converter topologies have been explored to meet the project parameters. DC buses can be connected to multiple power sources. Therefore, each source connected to this bus must have a converter. Isolation transformers allow separation between the input and output using switches [11].

Photovoltaic energy is one of the most widely used renewable energy sources owing to its availability and environmental advantages. There are a variety of uses. To be most efficient, PV systems must be kept at Maximum Power Point (MPP) by applying complete Power Point Tracking Technology (MPPT).

This automated control approach ensures that the SPV system operates at its MPP while taking into consideration environmental variables like as temperature, solar intensity, SPV characteristics, and component protection. This review focuses on the MPPT technique for reverse conversion of a photovoltaic separator. [12].

An improved windless control strategy is proposed for Photovoltaic (PV) systems coupled with DC-DC converters and three-phase inverters. The controller can withstand external interference, works well in various atmospheric conditions, and reduces the cooling components installed in the network.

The control scheme uses a Lyapunov function to ensure the stability of the system. Adaptive control measures are also implemented to improve the system's ability to withstand external shocks. To maximize the power output of the solar system, the additive control method and the DC-DC converter control strategy are applied. A three-phase inverter connected to the network using an LCL-type filter has also been adapted to the proposed control method [13].

This research investigates the converter's accomplishments, operating technique, stability and performance assessment and compares it to other converters in the same series. The MOSFET in the converter has a low Resistance State (RDS-ON), which minimizes conduction loss and operating factor. Furthermore, the low input current draw extends the life of the input PV panel and simplifies the achievement of the PV panel's Maximum Power Point (MPP).

To confirm the mathematical analysis's accuracy and the suggested structure's efficacy, a test model was developed with an input voltage of 20 V, an output voltage of 200 V, a rated power of 200 W, and an operating frequency of 50 kHz. The efficiency of the proposed converter was evaluated at different power levels and found to be greater than 95% [14].

The design incorporates a photovoltaic module, an ANFIS reference model, a DC-DC boost converter, and a control logic (FL) controller that sends a control signal to the converter. The simulation findings demonstrate the strength of this strategy since they indicate that the operator can extract the most energy possible under any weather circumstances.

The Pulsed and Observed (P&O) MPPT approach is compared to the AFIS-based MPPT control. This controller improves the photocell's power production by balancing the load resistance. Several MPPT techniques have been presented to achieve the optimal balance between PV components and load resistances [15].

A DC-DC power converter steps up the DC voltage from a low voltage to a high voltage. It uses active and passive components such as transistors, inductors, diodes and capacitors. The primary function of this converter is to generate a DC output voltage greater than the input voltage. This is accomplished by altering the duty cycle of the transistor's Pulse Width Modulation (PWM) switch, allowing both the inductor and the capacitor to be charged simultaneously.

The effectiveness of various DC-DC converter topologies has been studied in the context of photovoltaic power generation systems. However, special considerations must be made when choosing an appropriate topology for low-power photovoltaic applications. 7 of the 20 reviewed HGLP DC-DC converter topologies were selected as possible options [16].

AI integration is essential for effective MPPT monitoring during peak performance. Because the method is an AI-based MPPT approach, choosing one can be challenging. All AI methods show fast conversion, low drift, and high efficiency compared with traditional MPPT methods. However, AI-based MPPT methods require significant computing power and budget to implement. Hybrid MPPT combines the best features of AI-based MPPT methods with traditional methods, making it an effective strategy for achieving a trade-off between complexity and results [17].

Coupled inductors and capacitors are used in parallel for charging and discharging, resulting in a large increase in voltage. The power of the inductor flow allows two changes to achieve zero voltage transfer, thereby reducing and increasing efficiency. This reduces the stress on the valve and allows the use of lower-pressure units. The lab developed a prototype with 100W output using 25 V input and 380V output to evaluate the effectiveness of the converter. Detailed account working principle, stable operation and parameter configuration can reach 96.21% [18].

The previous work analysis examined the various losses that occur in both technical and non-technical aspects of transmission and distribution lines in a power system. Additionally, we also argued the losses that can occur in semi-conductive devices. The two main types of semiconductors used in electrical-semiconductor switches for inverters and electric appliances are MOSFETs and IGBTs. MOSFETs have a high switching frequency range and play a significant role in reducing losses, as explained below.

### *2.1. Power Losses*

Power losses occur as switching operations, and large transmissions occur in MOSFETs, depending on the switching component's PWM configuration and power source requirements. Whenever a switching state operates or changes, all chips lose power.

$$P_{\text{IGBT or MOSFET(AV)}} = P_{\text{Conduction losses}} + P_{\text{Switching losses}} \quad (1)$$

#### *2.1.1. Conduction Losses*

Conduction losses are the losses incurred when an unregulated MOSFET operates and conducts at a particular frequency. The on-state voltage combined with the on-state current produces the overall power dissipation during conduct. To calculate the average energy output in PWM usage, the conduction loss must be multiplied by the duty constant.

$$P_{cond(IGBT\ or\ MOSFET)} = \frac{1}{T} \int_0^T [V_{CE}(t) * I_{CE}(t)]\, dt \quad (2)$$

$$P_{cond(IGBT\ or\ MOSFET)} = [V_{CE}(t) * V_{CE}(t)]\ dt \quad (3)$$

#### *2.1.2. Switching Losses*

Switching losses are called the energy losses that transpire as the transistor switches between it is on and off modes. Transistors are semiconductors that undergo short periods of transition during which they go from the off-state (non-conducting) to the on state conduct. The semiconductor transistor functions in a zone where voltage and current fluctuate concurrently throughout this transition, which causes energy losses and power loss.

$$P_{sw-H} = \frac{1}{2} \times V_{IN} \times I_o \times (t_r + t_f) \times f_{sw}\,[w] \quad (4)$$

Where,
$V_{IN}$ - Input voltage,
$I_O$ - Output current
$t_r$ - High side MOSFET rise time
$t_f$ - High side MOSFET fall time
$f_{sw}$ - Switching Frequency (Hz)

## 3. Materials

Figure 1 represents the proposed block diagram consisting of a 12V PV input source, Battery 12V, MPPT using CNN, Selective Harmonic Elimination and VSI DC-AC inverter. The non-isolated DC-DC Converter is an interface that features two distinct modes of operation for soft-switching, therefore accommodating a wide variety of input voltages and mitigating strain on the switches and diodes.

This VSI operates in three modes: two for switch ON and one for switch OFF. In inverters that utilize PWM switching, the DC input voltage is typically consistent in magnitude and Selective Harmonic Elimination for switching state operation to reduce the harmonics distortion. Additionally, a metal-oxide-semiconductor field-effect transistor is employed, with a lower ON-state resistance compared to MOSFET switches.

### *3.1. PV Cell*

The photovoltaic effect is the process of conversion of light into electrical power. Essentially, a Photovoltaic cell is a type of p-n junction semiconductor that is an apparatus with an electrical characteristic based on I-V measurements obtained.

Figure 2 shows that a photovoltaic element has been recognized connection between $V_{in}$ input and $V_o$ output for each cell parameter estimation from parallel inductance or resistance. Comparing $I_c$ and $I_d$ measurements for losses of I-V measurements that the approach is a consistent and accurate voltage level increase and decrease estimate the current leakage, at the bottom of the n-type layer a current collector. When an electric field is applied, all particles, including photoelectrons, follow a straight path. These electrical fields exist in semiconductors, particularly photovoltaic (diode) junctions.

Where,
$V_{in}$ - Photovoltaics produced voltage,
$I_C$ - Capacitive current,
Id - Diode current,
$I_{out}$ - Output current.

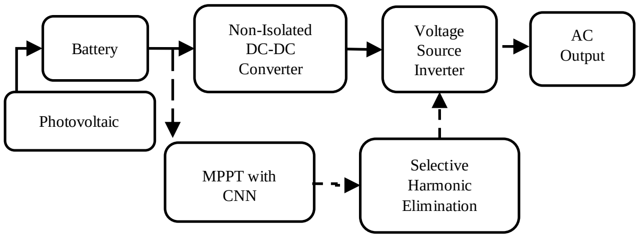


**Fig. 1 Block diagram of proposed PV VSI output**

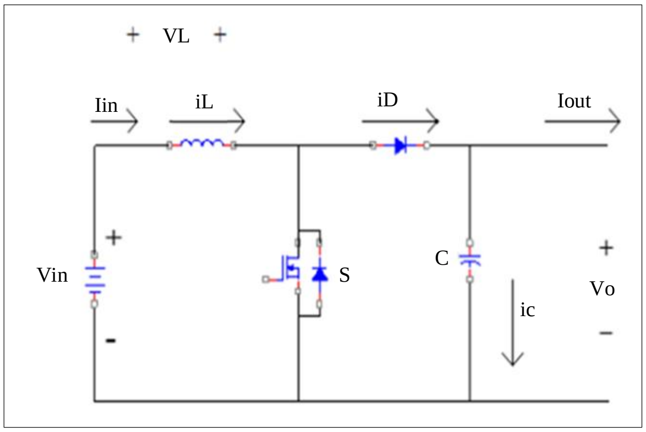


**Fig. 2 PV circuit operation**

## 4. Methodology

In this methodology, the operation of MPPT with CNN, a non-isolated DC-DC converter and a MOSFET-based DC-AC VSI inverter with selective harmonic elimination will be discussed below.

### *4.1. Maximum Power Point Tracking (MPPT) Using Convolutional Neural Network (CNN)*

The MPPT module is designed in three phases. In the first step, the basic PV module reads temperature and irradiance values from the solar panel and outputs the current value at MPP. The second stage entails data collecting based on the simulation findings from the preceding phase. Once the training dataset is ready, we can utilize it to train the proposed CNN and get the final output from our test data.

Figure 3 shows the workflow for the MPPT technique; it tracks the input solar DC voltage $V_{pv}$ and current $I_{pv}$ using MPPT for training and CNN for testing. MPPT utilizes the full performance of the PV module by controlling the voltage generated for the battery's charging condition. The charge controller maintains the voltage and current at the optimal level of battery level.

Figure 4 shows the MPPT using ANN, which is composed of inputs, a minimum of four hidden layers, and a Convolutional layer that tracks the hidden voltage. This max pooling layer tracks the error voltage, a dropout layer, and one output layer.

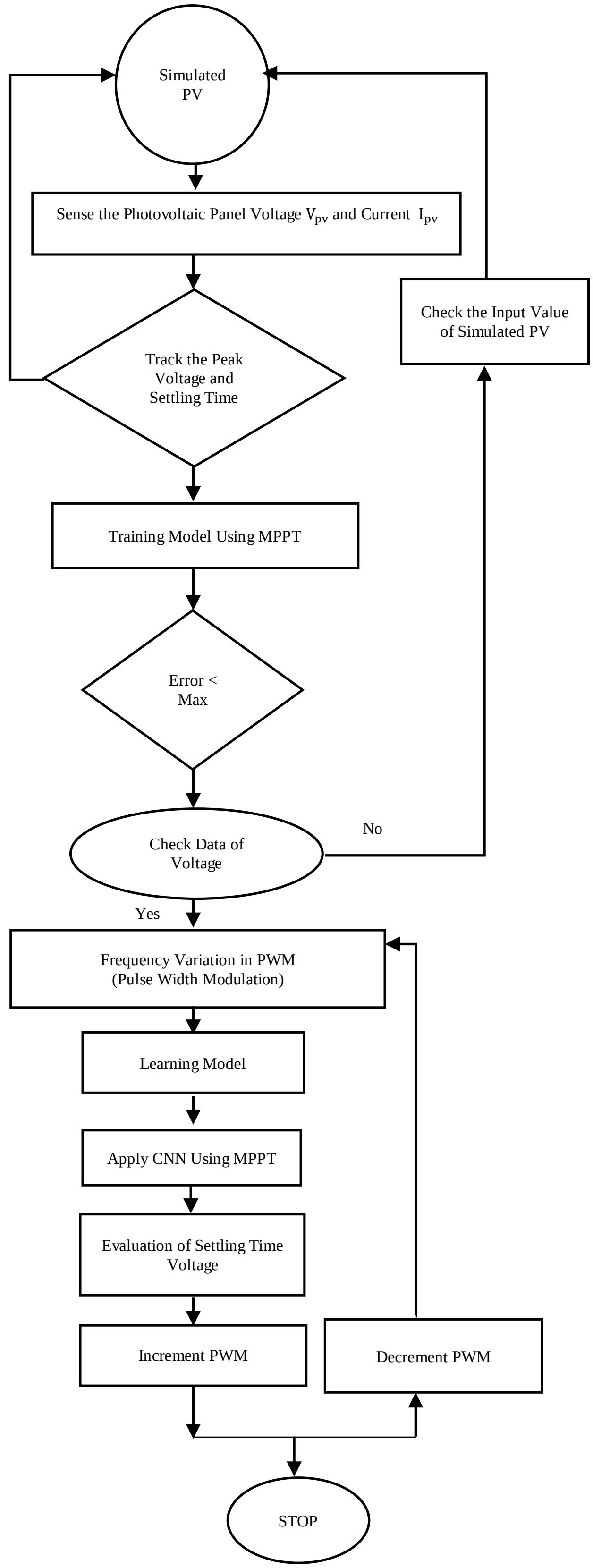


**Fig. 3 Flow chart MPPT using CNN**

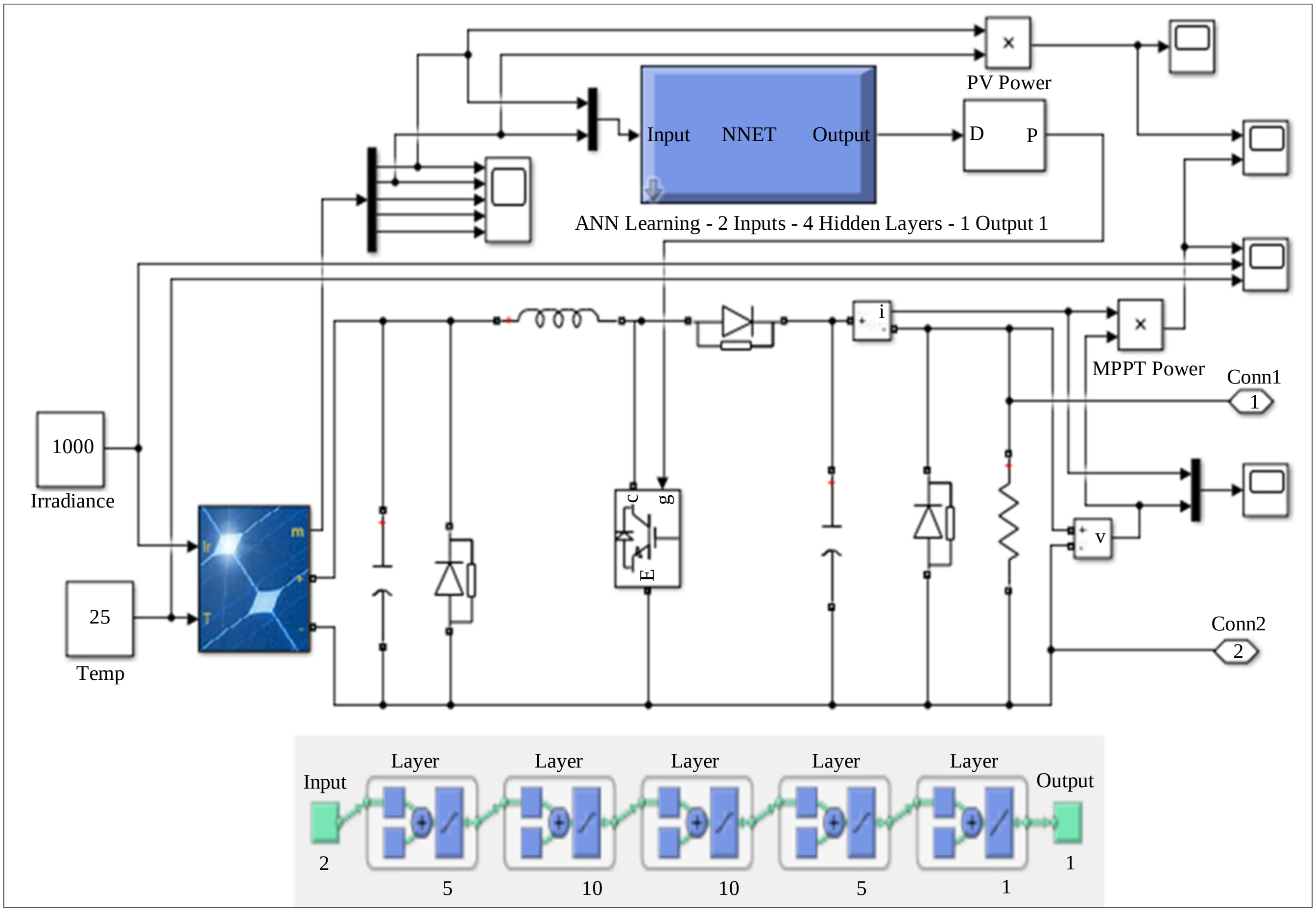


**Fig. 4 Simulation output of PV with MPTT and CNN**

### *4.2. Non-Isolated DC-DC Converter*

The inductance and clamp capacitor work together to deliver moderate switching, which lowers the stresses across the switch and improves efficiency at low power outputs. A parallel soft switching mechanism is incorporated with two Do and D1 diodes. The selected inductance and clamp capacitor work together to regulate the flow of current and reduce stress on the switch during moderate switching; this results in improved efficiency at low power outputs and reduced stress on the switch.

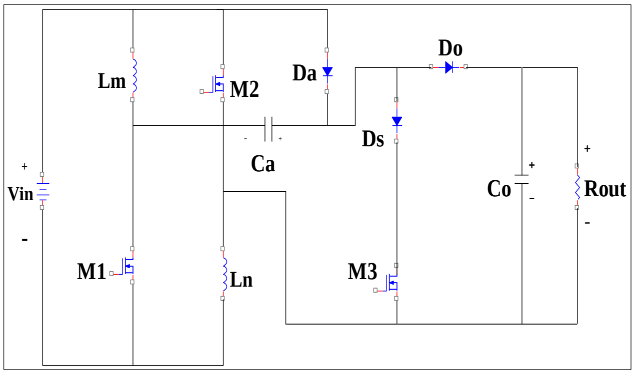


**Fig. 5 Circuit diagram of non-isolated DC-DC converter**

Figure 5 shows the components of the converter, including two capacitors (Ca and Co), two inductors (Lm and Ln), three diodes (Da, Ds, and Do), and three power semiconductor switches (M1, M2, and M3). The switching frequency of the converter is denoted as fs. The duty ratio of MOSFET switches M1 and M2 is represented by D1, while D2 represents the duty ratio of M3.

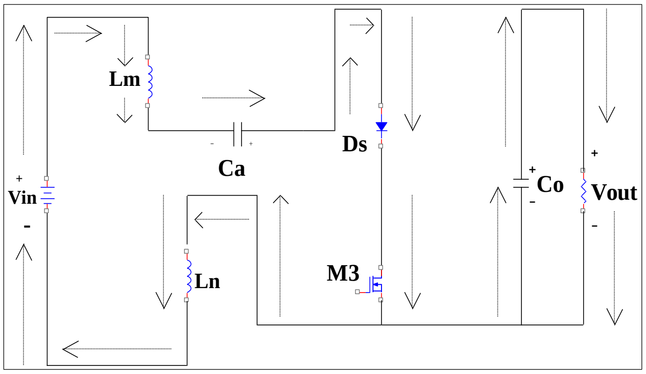


**Fig. 6 Mode I operation**

MOSFET M1 and M2 turn off simultaneously within the time range [t1 to t2], while MOSFET M3 is turned on. In

Figure 6 Mode I operation, the current flow path is shown as $V_{in}$, Ca, Ds, and Ln. The energy is delivered from the source to the capacitors and inductors in a specific order, and the voltage between MOSFETs M1 and M2 in this mode is approximately half of the input voltage from the source. The output capacitance Co powers the load impedance. $V_{out}$ When Ln is reversed, the input and opposite voltage are in series with the inductors Lm, Ln, and Ca.

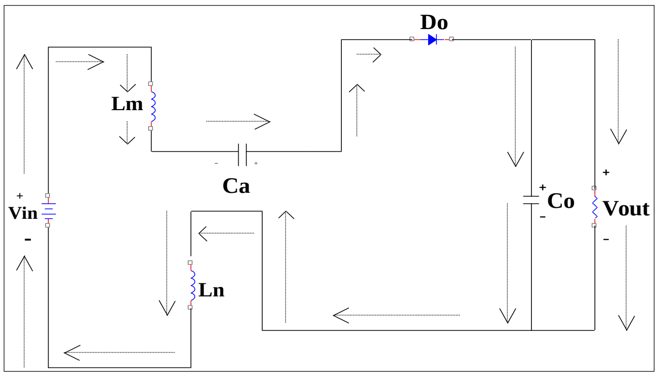


**Fig. 7 Mode II operation**

All three control semiconductor switches (M1, M2, and M3) are off during the interval [t2 to t3]. In Figure 7, this flow route is shown. In this mode, the load $V_{in}$ is supplied by the source and stored energy from the inductors and capacitors. The status of diodes Da and Ds is reverse-biased. The output capacitor Co is charged since Do is forward-biased in this mode. In this mode, the source and load are in series with inductors Lm, Ln, and capacitors Ca.

### *4.3. Voltage Source Inverter (VSI)*

One kind of converter that converts DC voltage to AC voltage is called a voltage source inverter. It converts a unidirectional voltage pattern into a sinusoidal voltage waveform, providing a steady voltage output. While the magnitude of the input DC voltage remains practically constant, the frequency and amplitude of the AC output voltage change. Therefore, the inverter must regulate both the amplitude and frequency of the output voltages.

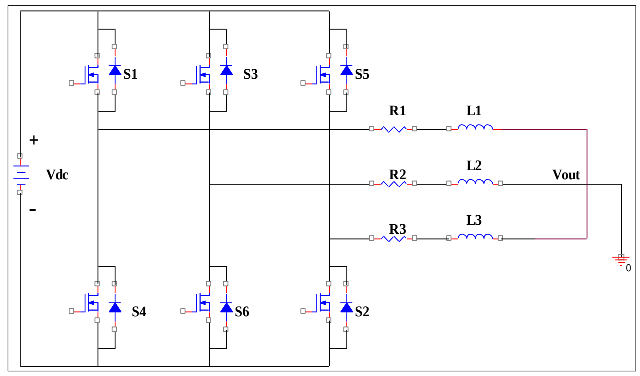


**Fig. 8 Circuit of DC-AC VSI inverter**

Figure 8 illustrates the three-terminal configuration of the six switches (S1 and S4, S3 and S6, S5 and S2), four-leg configuration. This configuration allows for the application of an MPPT-based PWM condition based on frequency variation at the input gate terminal. The voltage source inverter that uses the MPWM switching technique has a DC input voltage ($V_{dc}$= 12V to 24V) connected to the middle point of the RL load.

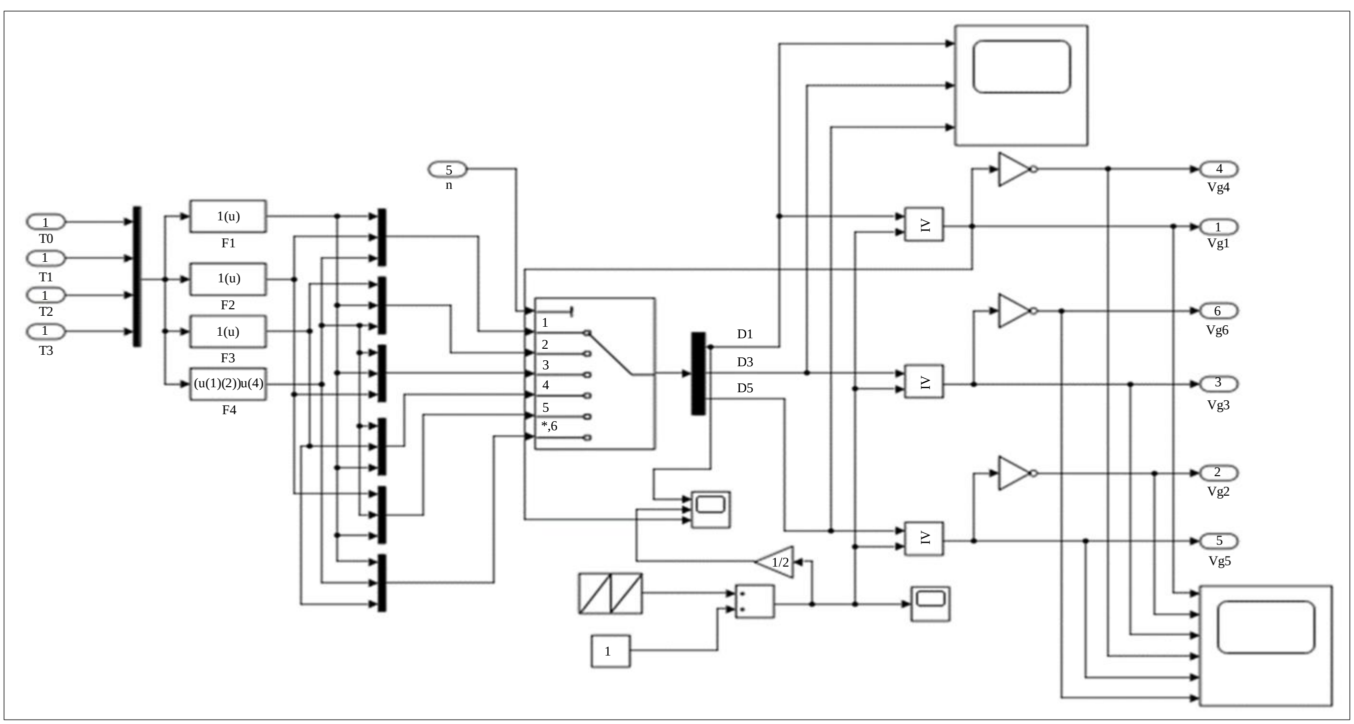


**Fig. 9 Simulation circuit of VSI inverter switching state operation**

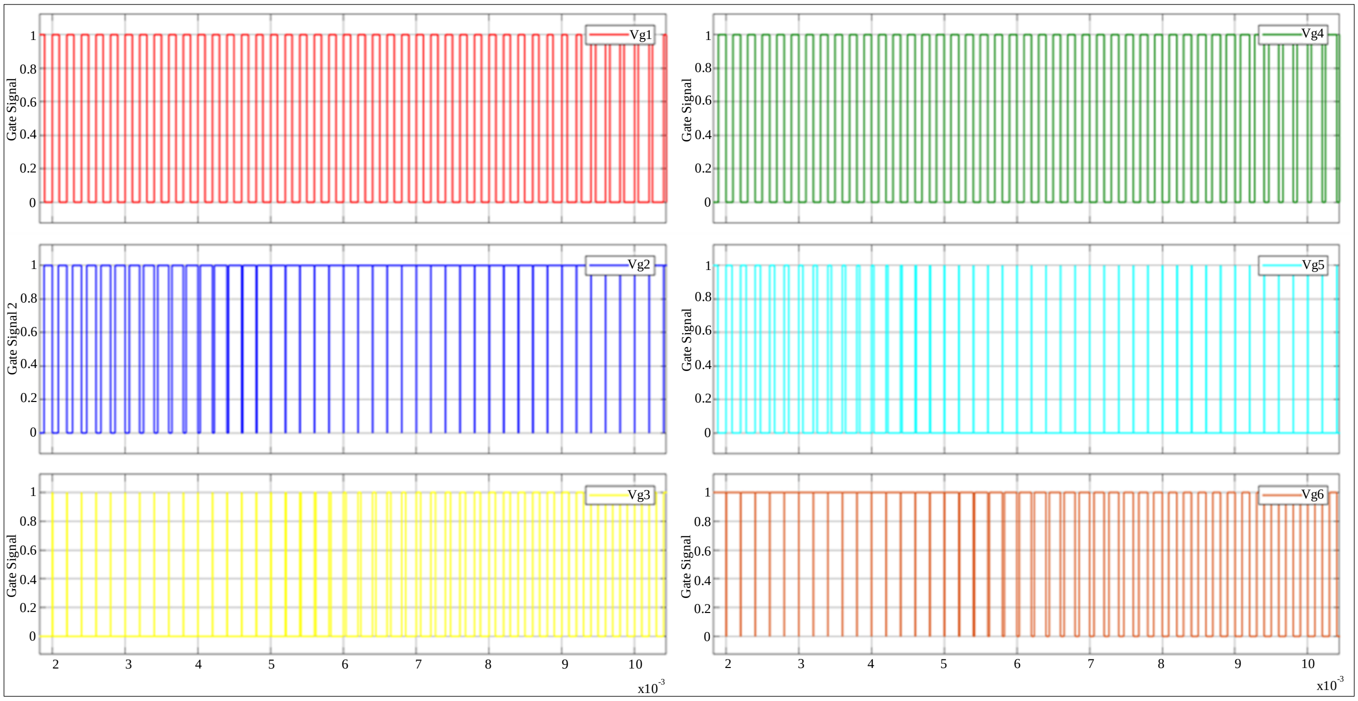


**Fig. 10 Selective harmonic elimination waveform of six switches (S1 and S4, S3 and S6, S5 and S2) in VSI**

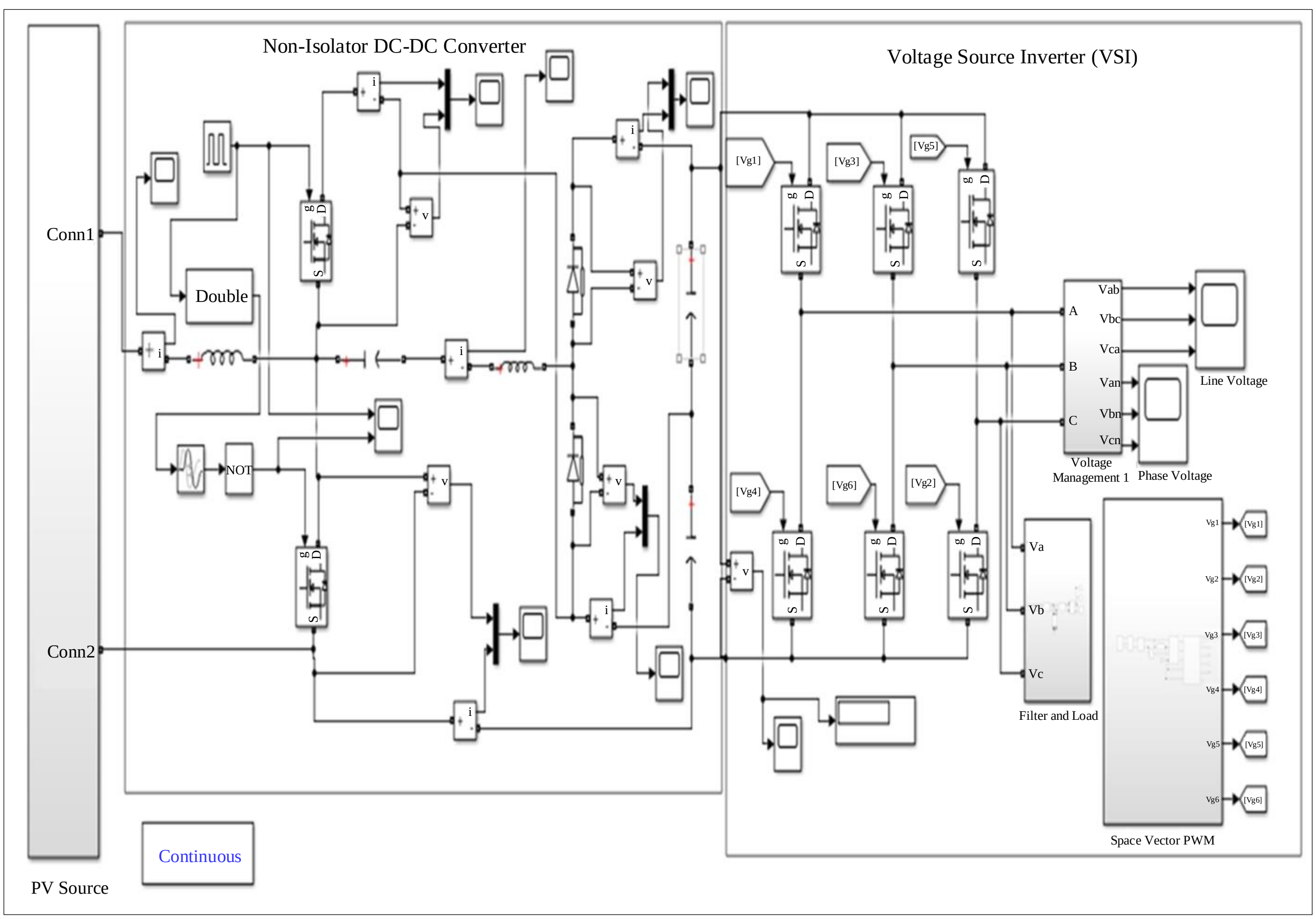


**Fig. 11 PV and VSI inverter with MOSFET switch device**

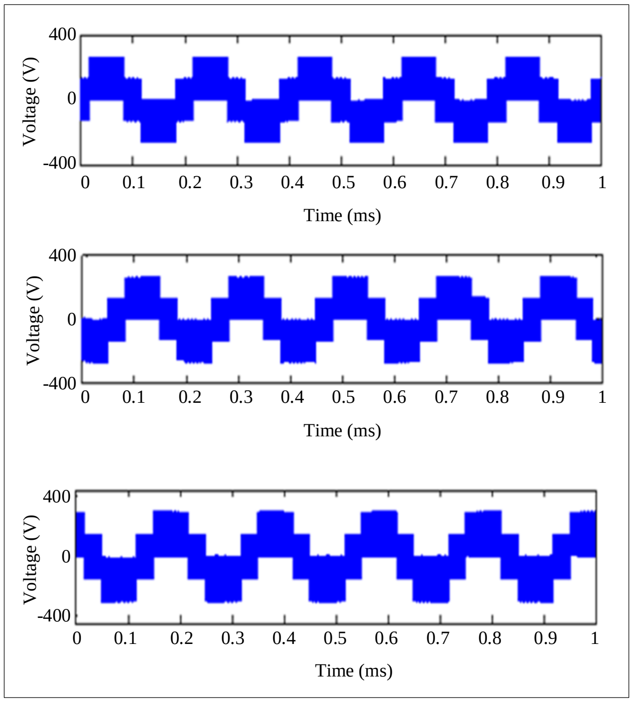


**Fig. 12 Phase voltage with PWM output**

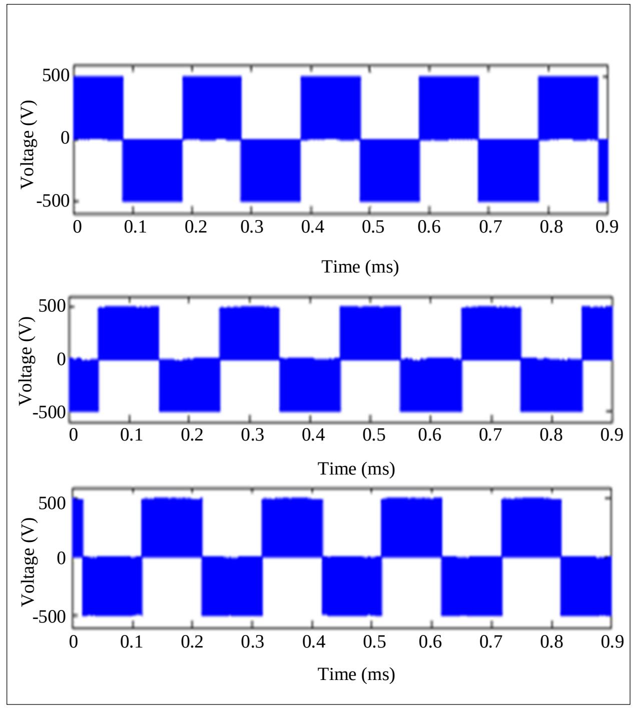


**Fig. 13 Line voltage with PWM output**

*4.3.1. Selective Harmonic Elimination*

Figure 9 shows the Selective Harmonic Elimination Switching state operation analytical model assumes that a capacitor on the DC side provides a stable DC voltage. Each switch operation has an anti-parallel sinusoidal, rectangular output that allows current to flow in the opposite direction.

This method applies an MPPT-based PWM condition to regulate the VSI output voltage for reducing losses in conduction and power transfer, it transfers voltage from the VSI converter to the grid. Figure 10 displays the output waveform of MSPWM S1, S4, and S5 are closed from 0 to 60, while the other four switches are open. S1, S4, and S6 are closed from 60 to 120, while the other four switches are open. S1, S3, and S6 are closed from 120 to 180, while the other four switches are open.

## 5. Results and Discussion

Figure 11 shows the simulation proposed method contains line inductance and resistance of 0.001H and 0.001 Ω, load resistance of 100 Ω with a capacitance of 1000 µF, and other parameters were utilized in all three simulations. 12 V DC supply voltage at 50 Hz Fr and 1 kHz Fs is available, and the modulation index is set to 0.1 and the gain factor to 1.

In Figure 12, the voltage VIP= 410.5 is depicted along a voltage instability predictor in a source or load with three different phases. Finally, Figure 13 illustrates the V0P= 405.6 for peak value among any three-phase system, which is recognized as the voltage at the line.

Table 1 shows a comparison of two different inverter techniques using MOSFET operation, which indicates a reduction in conduction losses.

### *5.1. Output Comparison*

Figure 14 shows that the VSI inverter output with efficiency evaluation with the MOSFET is 0.8% more efficient than that with the MOSFET, as shown in Figure 15.

**Table 1. Comparison of two different inverters**

| Switch Device MOSFET | $V_{IP}$ (Phase Voltage) | $V_{0P}$ (Line Voltage) | $V_D$ (Voltage Drop) | Total $V_D$(v) |
|---|---|---|---|---|
| Proposed VSI | 410.5 | 408.6 | 2.265 | 4.786 |
| Existing Inverter | 339.9 | 331.2 | 3.112 | 6.224 |

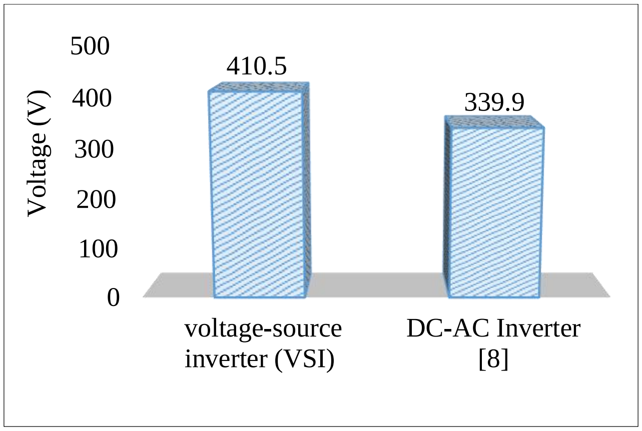


**Fig. 14 Inverter output voltage**

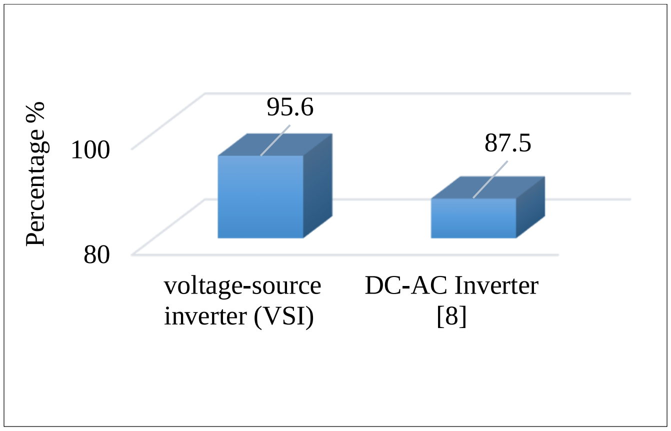


**Fig. 15 Efficiency comparison evaluation of the inverters**

## 6. Conclusion

This conclusion discusses the use of a CNN-based MPPT technique to improve the efficiency and reduce switching losses in a MOSFET in both a converter and inverter. A Three Phase Voltage Source Inverter (VSI) is used to transform the DC input voltage into a three-phase variable frequency adjustable voltage output. Selective harmonic elimination is then used to eliminate specified low-order harmonics from the voltage/current waveform. The MOSFET switching device and resonating component are coupled in series, resulting in a decrease in linear and phase voltage analyses through each switching device to zero, improving the circuit's fundamental features. The output results show an improved efficiency of 96% and reduced voltage variation, resulting in improved energy efficiency during switching state operation. In the future, this technique will be applied to different loads with different inverter techniques to analyze various loss conditions.

## References

[1] Syed Muhammad Ahsan et al., "Harmonic Analysis of Grid-Connected Solar PV Systems with Nonlinear Household Loads in Low-Voltage Distribution Networks," *Sustainability*, vol. 13, no. 7, pp. 1-23, 2021. [CrossRef] [Google Scholar] [Publisher Link]

[2] Rayappa David Amar Raj, Thabeti Aditya, and Madhav Ramrao Shinde, "Power Quality Enhancement of Grid-Connected Solar Photovoltaic System Using LCL Filter," *2020 International Conference on Power Electronics & IoT Applications in Renewable Energy and its Control (PARC)*, India, pp. 334-339, 2020. [CrossRef] [Google Scholar] [Publisher Link]

[3] CH Hussaian Basha, and C. Rani, "Different Conventional and Soft Computing MPPT Techniques for Solar PV Systems with High Step-Up Boost Converters: A Comprehensive analysis," *Energies*, vol. 13, no. 2, pp. 1-27, 2020. [CrossRef] [Google Scholar] [Publisher Link]

[4] Issa Batarseh, and Ahmad Harb, *Soft-Switching DC-DC Converters*, Power Electronics, Springer eBooks, pp. 347-460, 2017. [CrossRef] [Google Scholar] [Publisher Link]

[5] Catalina González-Castaño et al., "MPPT Algorithm Based on Artificial Bee Colony for PV System," *IEEE Access*, vol. 9, pp. 43121-43133, 2021. [CrossRef] [Google Scholar] [Publisher Link]

[6] Ke Guo et al., "An Improved Gray Wolf Optimizer MPPT Algorithm for PV System with BFBIC Converter under Partial Shading," *IEEE Access*, vol. 8, pp. 103476-103490, 2020. [CrossRef] [Google Scholar] [Publisher Link]

[7] Shreyas Rajendra Hole, and Agam Das Goswami, "Quantitative Analysis of DC-DC Converter Models: A Statistical Perspective Based on Solar Photovoltaic Power Storage," *Energy Harvesting and Systems*, vol. 9, no. 1, pp. 113-121, 2022. [CrossRef] [Google Scholar] [Publisher Link]

[8] Md Tariqul Islam et al., "A Novel Asymmetric Multi-level Inverter with Phase Disposed Switching Technique for Grid Integration of Solar Photovoltaic Systems," *2020 IEEE Region 10 Symposium (TENSYMP)*, Bangladesh, pp. 726-729, 2020. [CrossRef] [Google Scholar] [Publisher Link]

[9] Rashid Ahmed Khan et al., "A Novel High-Voltage Gain Step-Up DC-DC Converter with Maximum Power Point Tracker for Solar Photovoltaic Systems," *Processes*, vol. 11, no. 4, pp. 1-23, 2023. [CrossRef] [Google Scholar] [Publisher Link]

[10] Kotb M. Kotb et al., "Enriching the Stability of Solar/Wind DC Microgrids Using Battery and Superconducting Magnetic Energy Storage Based Fuzzy Logic Control," *Journal of Energy Storage*, vol. 45, 2022. [CrossRef] [Google Scholar] [Publisher Link]

[11] Md. Masudur Rahman et al., "An Advanced Nonlinear Controller for the LCL-Type Three-Phase Grid-Connected Solar Photovoltaic System with a DC-DC Converter," *IEEE Systems Journal*, vol. 16, no. 2, pp. 3203-3214, 2022. [CrossRef] [Google Scholar] [Publisher Link]

[12] Pawan Kumar Pathak, Anil Kumar Yadav, and P.A. Alvi, "Advanced Solar MPPT Techniques Under Uniform and Non-Uniform Irradiance: A Comprehensive Review," *Journal of Solar Energy Engineering*, vol. 142, no. 4, pp. 1-26, 2020. [CrossRef] [Google Scholar] [Publisher Link]

[13] Chaoping Rao et al., "A Novel High-Gain Soft-Switching DC-DC Converter with Improved P&O MPPT for Photovoltaic Applications," *IEEE Access*, vol. 9, pp. 58790-58806, 2021. [CrossRef] [Google Scholar] [Publisher Link]

[14] Saibal Manna et al., "Design and Implementation of a New Adaptive MPPT Controller for Solar PV Systems," *Energy Reports*, vol. 9, pp. 1818-1829, 2023. [CrossRef] [Google Scholar] [Publisher Link]

[15] Abhinav Saxena et al., "Maximum Power Extraction from Solar PV Systems Using Intelligent Based Soft Computing Strategies: A Critical Review and Comprehensive Performance Analysis," *Heliyon*, vol. 10, no. 2, 2023. [CrossRef] [Google Scholar] [Publisher Link]

[16] Libin Xu, Ruofa Cheng, and Jiajing Yang, "A New MPPT Technique for Fast and Efficient Tracking under Fast Varying Solar Irradiation and Load Resistance," *International Journal of Photoenergy*, vol. 2020, pp. 1-18, 2020. [CrossRef] [Google Scholar] [Publisher Link]

[17] Kah Yung Yap, Charles R. Sarimuthu, and Joanne Mun-Yee Lim, "Artificial Intelligence Based MPPT Techniques for Solar Power System: A review," *Journal of Modern Power Systems and Clean Energy*, vol. 8, no. 6, pp. 1043-1059, 2020. [CrossRef] [Google Scholar] [Publisher Link]

[18] Xiangjun Zhang et al., "Novel High Step-Up Soft-Switching DC-DC Converter Based on Switched Capacitor and Coupled Inductor," *IEEE Transactions on Power Electronics*, vol. 35, no. 9, pp. 9471-9481, 2020. [CrossRef] [Google Scholar] [Publisher Link]